Cornell University
Mechanical & Aerospace Engineering
Raymond Corporation Project

Fall 2013

Reach Truck Forklift Model

Nathan Woo (nw269), Mechanical Engineering, M.Eng., '14
Alais Hewes (amh299), Mechanical Engineering, B.S., '14
Megan Gould (mmg99), Mechanical Engineering, B.S., '14
Professor Ephrahim Garcia, Ph.D., Academic Project Advisor
Fernando Goncalves, Ph.D., Industry Coordinator

A mathematical model has been developed to capture the dynamics of the Raymond Corporation Reach Truck forklift. The development of this model has been made possible by a combination of analytical and experimental technques for parameter identification and system modeling. This mathematical model was used as a frame of study for developing a control system to increase system performance.

Objective

Raymond's Reach Truck forklift can be subject to considerably large oscillations caused by accelerating or decelerating the tractor. These undesirable oscillations are especially prevalent when the payload is large, and the carriage carrying the payload is elevated. Reducing these oscillations would lead to improved productivity and reduced anxiety of the operator. The primary project objective was to develop a mathematical model for the reach truck using system modeling and parameter identification techniques. The mathematical model was and will be used to develop feedback control strategies to attenuate mast oscillations and optimize system performance. A secondary project objective was to investigate the reaction of the mast and the payload and carriage when the forklift turns.

The reach truck was modeled using two different techniques: a continuous mass model approach and lumped mass-spring-damper system approach. The transient response of the latter model was simulated and experimentally validated by comparing it to the empirical natural frequency. An initial control strategy featuring an electronically implemented dashpot was developed but proved not to be effective. Currently, a control strategy using a proof mass actuator system is being studied.

Approach

System Modeling

The forklift analyzed was a Raymond's Reach Truck depicted in the figure below. The reach truck is made up of three key components. The tractor at the base, which drives the reach truck, the carriage on which the payload is placed, and the mast, which allows the carriage to move up and down. The mast is made up of C-Channel at the base, and two smaller I-beam telescopes. When the telescopes are fully extended the mast is several meters high.

Figure 1: Physical image of Raymond's reach truck with key components of the model identified

Continuous Mast Model

An analytical model featuring a mast modeled as a continuously distributed beam was developed. To find the equations of motion, a Lagrangian formulation was developed for this model.
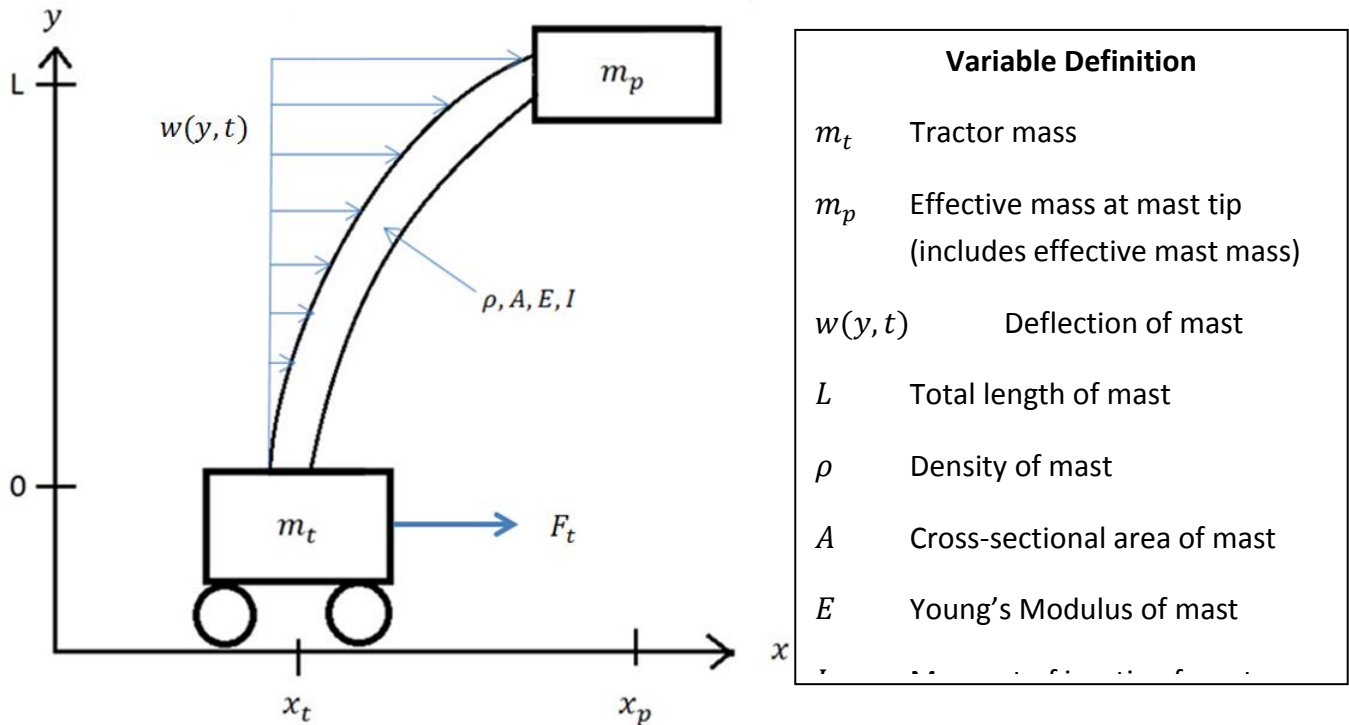

Variable Definition	
m_t	Tractor mass
m_p	Effective mass at mast tip (includes effective mast mass)
$w(y,t)$	Deflection of mast
L	Total length of mast
ρ	Density of mast
A	Cross-sectional area of mast
E	Young's Modulus of mast

Figure 2: Continuous mast model

The kinetic and potential energies of the system are

$$KE = \frac{1}{2}m_t\dot{x_t}^2 + \frac{1}{2}m_p\big(\dot{x}_t + \dot{w}(L,t)\big)^2 + \frac{1}{2}\int_0^L \rho A\big(\dot{x}_t + \dot{w}(y,t)\big)^2 dy$$

$$PE = \frac{1}{2}\int_0^L EI\left(\frac{d^2w}{dy^2}\right)^2 dy = \int_0^L EI(w''(y))^2 dy$$

We can apply separation of variables to the displacement $w(y,t)$.

$$w(y,t) = \sum_i \phi_i(y)q_i(t)$$

Where ϕ_i is the mode shape, and q_i is the displacement associated with that mode shape. The mast can be viewed as a cantilevered beam, with the following boundary conditions:

$$w(0,t) = 0$$

$$\frac{dw(0,t)}{dy} = 0$$

$$\frac{d^2w(L,t)}{dy^2} = 0$$

$$\frac{d^3w(L,t)}{dy^3} = 0$$

From these boundary conditions, we can derive the mode shape for a cantilevered beam.

$$\phi_n(y) = A_1\left[\cosh\beta_n y - \cos\beta_n y + \frac{(\cos\beta_n L + \cosh\beta_n L)(\sin\beta_n y - \sinh\beta_n y)}{\sin\beta_n L + \sinh\beta_n L}\right]$$

Where A_1 is an arbitrary displacement amplitude and $\beta_n L$ are roots to the equation

$$\cosh(\beta_n L)\cos(\beta_n L) + 1 = 0$$

Assume we can approximate the displacement as a single vibrational mode.

$$w(y,t) = \phi_1(y)q_1(t)$$

The energy terms then become

$$KE = \frac{1}{2}m_t\dot{x_t}^2 + \frac{1}{2}m_p\big(\dot{x}_t + \phi_1(y)\dot{q}_1(t)\big)^2 + \frac{1}{2}\int_0^L \rho A\big(\dot{x}_t + \phi_1(y)\dot{q}_1(t)\big)^2 dy$$

$$KE = \frac{1}{2}m_t\dot{x_t}^2 + \frac{1}{2}m_p\big(\dot{x}_t + \phi_1(y)\dot{q}_1(t)\big)^2 + \frac{1}{2}\int_0^L \rho A\, dy * \dot{x}_t^2$$

$$+ \int_0^L \rho A\phi_1(y)dy * \dot{x}_t\dot{q}_1(t) + \frac{1}{2}\int_0^L \rho A\phi_1^2(y)dy * \dot{q}_1^2(t)$$

$$KE = \frac{1}{2}m_t\dot{x}_t{}^2 + \frac{1}{2}m_p\big(\dot{x}_t + \phi_1(y)\dot{q}_1(t)\big)^2 + \frac{1}{2}\int_0^L \rho A\, dy * \dot{x}_t^2$$

$$+ \int_0^L \rho A\phi_1(y)dy * \dot{x}_t\dot{q}_1(t) + \frac{1}{2}\int_0^L \rho A\phi_1^2(y)dy * \dot{q}_1^2(t)$$

$$PE = \frac{1}{2}\int_0^L EI(\phi_1''(y))^2 dy * q_1^2(t)$$

Therefore, the Lagrangian is

$$\mathcal{L} = KE - PE = \frac{1}{2}m_t\dot{x}_t{}^2 + \frac{1}{2}m_p\big(\dot{x}_t + \phi_1(y)\dot{q}_1(t)\big)^2 + \frac{1}{2}\int_0^L \rho A\, dy * \dot{x}_t^2$$

$$+ \int_0^L \rho A\phi_1(y)dy * \dot{x}_t\dot{q}_1(t) + \frac{1}{2}\int_0^L \rho A\phi_1^2(y)dy * \dot{q}_1^2(t) - \frac{1}{2}\int_0^L EI(\phi_1''(y))^2 dy * q_1^2(t)$$

We must examine two general coordinates for the Lagrangian formulation: $x_t(t)$ and $q_1(t)$. This yields two Lagrange equations

$$-\frac{\partial\mathcal{L}}{\partial x_t} + \frac{d}{dt}\left(\frac{\partial\mathcal{L}}{\partial \dot{x}_t}\right) = F_t$$

$$-\frac{\partial\mathcal{L}}{\partial q_1} + \frac{d}{dt}\left(\frac{\partial\mathcal{L}}{\partial \dot{q}_1}\right) = 0$$

Evaluating each derivative yields

$$\frac{\partial\mathcal{L}}{\partial x_t} = 0$$

$$\frac{\partial\mathcal{L}}{\partial \dot{x}_t} = m_t\dot{x}_t + m_p\big(\dot{x}_t + \phi_1(L)\dot{q}_1(t)\big) + \int_0^L \rho A\, dy * \dot{x}_t + \int_0^L \rho A\phi_1(y)dy * \dot{q}_1(t)$$

$$= \left(m_t + m_p + \int_0^L \rho A\, dy\right)\dot{x}_t + \left(m_p\phi_1(L) + \int_0^L \rho A\phi_1(y)dy\right)\dot{q}_1(t)$$

$$\frac{\partial\mathcal{L}}{\partial q_1} = \int_0^L EI(\phi_1''(y))^2 dy * q_1(t)$$

$$\frac{\partial\mathcal{L}}{\partial \dot{q}_1} = m_p\big(\dot{x}_t + \phi_1(L)\dot{q}_1(t)\big)\phi_1(L) + \int_0^L \rho A\phi_1(L)dy * \dot{x}_t + \int_0^L \rho A\phi_1^2(L)dy * \dot{q}_1(t)$$

$$= \left(m_p\phi_1(L) + \int_0^L \rho A\phi_1(y)dy\right)\dot{x}_t + \left(m_p\phi_1^2(L) + \int_0^L \rho A\phi_1^2(y)dy\right)\dot{q}_1(t)$$

Thus, the two equations of motion are

$$\left(m_t + m_p + \int_0^L \rho A\, dy\right)\ddot{x}_t + \left(m_p\phi_1(L) + \int_0^L \rho A\phi_1(y)dy\right)\ddot{q}_1 = F_t$$

$$\left(m_p\phi_1(L) + \int_0^L \rho A\phi_1(y)dy\right)\ddot{x}_t + \left(m_p\phi_1^2(L) + \int_0^L \rho A\phi_1^2(y)dy\right)\ddot{q}_1 - \left(\int_0^L EI\big(\phi_1''(y)\big)^2 dy\right)q_1 = 0$$

Written in matrix form, the equations of motion are

$$\begin{bmatrix} m_t + m_p + \int_0^L \rho A dy & m_p\phi_1(L) + \int_0^L \rho A\phi_1(y)dy \\ m_p\phi_1(L) + \int_0^L \rho A\phi_1(y)dy & m_p\phi_1^2(L) + \int_0^L \rho A\phi_1^2(y)dy \end{bmatrix} \begin{bmatrix} \ddot{x}_t \\ \ddot{q}_1 \end{bmatrix} + \begin{bmatrix} 0 & 0 \\ 0 & -\int_0^L EI\big(\phi_1''(y)\big)^2 dy \end{bmatrix} \begin{bmatrix} x_t \\ q_1 \end{bmatrix}$$
$$= \begin{bmatrix} 1 \\ 0 \end{bmatrix} F_t$$

Assuming orthonormal $\phi(y)$,

$$\int_0^L \rho A\phi_1^2(y)dy = 1$$

$$-\int_0^L EI\big(\phi_1''(y)\big)^2 dy = \omega_1^2$$

Furthermore,

$$\int_0^L \rho A dy = m_{mast}$$

Then the equations of motion become

$$\begin{bmatrix} m_t + m_p + m_{mast} & m_p\phi_1(L) + \int_0^L \rho A\phi_1(y)dy \\ m_p\phi_1(L) + \int_0^L \rho A\phi_1(y)dy & m_p\phi_1^2(L) + 1 \end{bmatrix} \begin{bmatrix} \ddot{x}_t \\ \ddot{q}_1 \end{bmatrix} + \begin{bmatrix} 0 & 0 \\ 0 & \omega_1^2 \end{bmatrix} \begin{bmatrix} x_t \\ q_1 \end{bmatrix} = \begin{bmatrix} 1 \\ 0 \end{bmatrix} F_t$$

The final form of the Lagrangian formulation can then be expressed as

$$M\ddot{\vec{x}} + K\vec{x} = B_f u$$

Two Degree of Freedom Lumped Mass Mode

The forklift was also modeled as a simple two degree of freedom lumped mass spring-damper system in order to begin developing simple control strategies. The continuous and distributed masses on the forklift were lumped into two distinct masses: m_t, the mass of the tractor, and m_m, which is the sum of the mass of the payload, carriage and 1/3 of the mass of the mast. The factor of 1/3 comes from redefining the mass of the mast at its tip rather than at its center of gravity. The forcing f applied to the system was

assumed to be the operator controlled acceleration required to move the tractor.
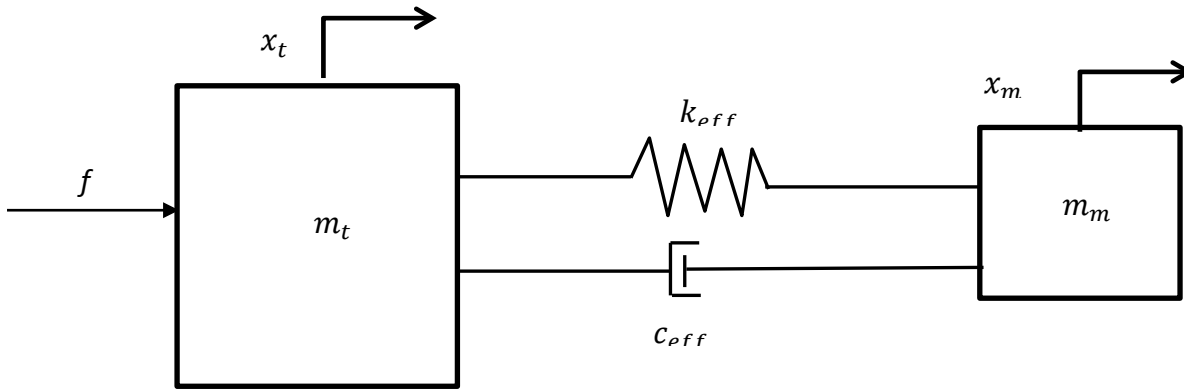
Figure 3: Lumped mass two degree of freedom spring-damper system

The equations of motion derived from a force balance on the system are

$$m_t \ddot{x}_t = k_{eff}(x_m - x_t) + c_{eff}(\dot{x}_m - \dot{x}_t) + f$$

$$m_m \ddot{x}_m = k_{eff}(x_t - x_m) + c_{eff}(\dot{x}_t - \dot{x}_m)$$

Where m_t is the mass of the tractor, m_m is the effective mass at the tip, x_t is the position of the tractor, x_m is the position of the tip of the mast, k_m is the effective stiffness of the mast and c_m is the effective damping of the mast.

These equations can additionally be expressed in matrix form as shown below

$$M\ddot{x} + C\dot{x} + Kx = \begin{bmatrix} m_t & 0 \\ 0 & m_m \end{bmatrix} \ddot{x} + \begin{bmatrix} c_{eff} & -c_{eff} \\ -c_{eff} & c_{eff} \end{bmatrix} \dot{x} + \begin{bmatrix} k_{eff} & -k_{eff} \\ -k_{eff} & k_{eff} \end{bmatrix} \dot{x} = \begin{bmatrix} f(t) \\ 0 \end{bmatrix}$$

Rearranging the equation of motions of the system, a state space system can be derived to model the system.

$$\begin{bmatrix} \dot{x}_t \\ \ddot{x}_t \\ \dot{x}_m \\ \ddot{x}_m \end{bmatrix} = \begin{bmatrix} 0 & 1 & 0 & 0 \\ -\dfrac{k_{eff}}{m_t} & -\dfrac{c_{eff}}{m_t} & \dfrac{k_{eff}}{m_t} & \dfrac{c_{eff}}{m_t} \\ 0 & 0 & 0 & 1 \\ \dfrac{k_{eff}}{m_m} & \dfrac{c_{eff}}{m_m} & -\dfrac{k_{eff}}{m_m} & -\dfrac{c_{eff}}{m_m} \end{bmatrix} \begin{bmatrix} x_t \\ \dot{x}_t \\ x_m \\ \dot{x}_m \end{bmatrix} + \begin{bmatrix} 0 \\ 1 \\ 0 \\ 0 \end{bmatrix} u$$

$$y = \begin{bmatrix} -1 & 0 & 1 & 0 \end{bmatrix} \begin{bmatrix} x_t \\ \dot{x}_t \\ x_m \\ \dot{x}_m \end{bmatrix} + 0$$

The input to the state space model u, is user defined and can be made to reflect whatever desired input is necessary for modeling (i.e. constant acceleration to tractor, continuous acceleration profile at the base of the tractor etc.) The output to the state space model y, is defined as the displacement between the

tractor and the mas at the tip of the mast, since the eventual project goals are to minimize this displacement. Although values for the masses are known, the effective stiffness and damping coefficient are not. The next step in modeling the system was to develop values for these coefficients.

Effective Stiffness and Damping Calculations

The effective stiffness of the mast was initially calculated using geometric and material data for the C-channel and I-beams composing the mast. Values for the moments of inertia and lengths of these beams are listed in Table 1 of the Appendix. The stiffness coefficient for each beam was found individually by treating each beam as a spring and solving for the stiffness. An effective coefficient of the entire mast was found by adding the stiffness coefficients of each beam in series. Both of the I-beams were assumed to be rigidly attached to the member below so that the slope and deflection at each of the interfaces was 0.
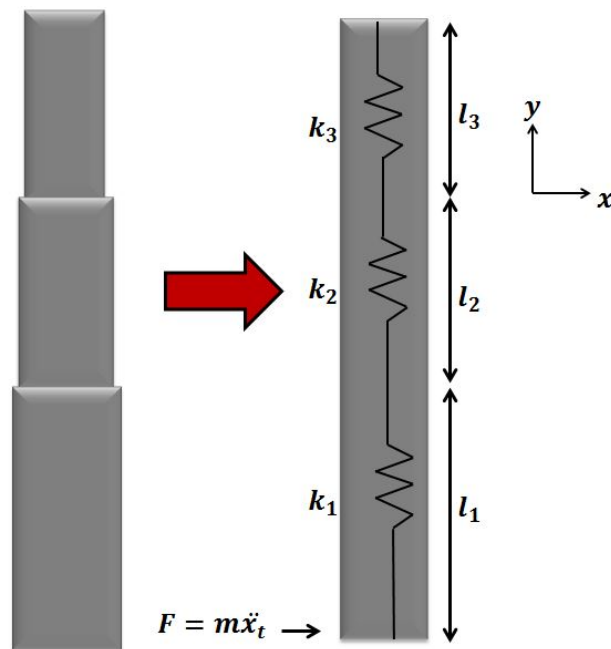
Figure 3: Model of Mast Base and Two Telescopes as a Cantilever Beam with Three Springs in Series

The stiffness was derived from the deflection of the mast. An expression for the deflection of the mast was found by first solving for the moments along the length of the mast and then integrating the flexure formula. The equation found for the moment was the following,

$$M(y) = Fy$$

Where F is the force of the moving tractor and y is the vertical distance from the base of the mast. The flexure formula is defined as,

$$EI\frac{d^2x}{dy^2} = M(y)$$

8

where E is the Young's modulus, I is the second area moment of inertia of the mast, and x is the deflection. After integrating the flexure formula twice we had the following arbitrary expression for the mast deflection,

$$x = \frac{F}{EI}\left(\left(\frac{1}{2}\right)Ly^2 - \left(\frac{1}{6}\right)y^3\right) + C_1 y + C_2$$

where C_1 and C_2 are the constants of integration. Using the boundary conditions $x(0) = 0$ and $\frac{dy}{dx}(0) = 0$ the following solution for the displacement was obtained

$$x(y) = \left(\frac{F}{3EI}\right)L^3 \rightarrow \left(\frac{3EI}{L^3}\right)x = F$$

By solving for the force and comparing the form of the equation to Hooke's law, the following stiffness was found,

$$k = \frac{L^3}{3EI}$$

Modeling the three beams as three springs in series, the total effective stiffness for the mast is given below

$$k_{eff} = \frac{k_1 k_2 k_3}{k_1 k_2 + k_2 k_3 + k_3 k_1}$$

The effective damping coefficient of the mast was computed from experimental data given in Fernando Goncalves' report on the Orderpicker Longitudinal Mast Dynamics. This was done by experimentally recording the transient response of the mast tip and finding the logarithmic decrement to find the system's natural frequency and damping ratio. Although values for the natural frequency and damping ratio were given in the Orderpicker Longitudinal Mast Dynamics report for the reach truck under various loading conditions with the carriage at different heights, the damping ratio can also be found from the following equation

$$\zeta = \frac{\delta}{\sqrt{4\pi^2 + \delta^2}}$$

And δ is the logarithmic decrement defined by

$$\delta = \ln\frac{x(t)}{x(t+T)}$$

Where x is the value of the experimental deflection at time t and T is the period of oscillation. The natural frequency can either be found by generating a normalized frequency power spectrum or by using the damping ratio ζ and damped natural frequency ω_d

$$\omega_n = \frac{\omega_d}{\sqrt{1 - \zeta^2}}$$

$$\omega_d = \frac{2\pi}{T}$$

Once values for the damping ratio and natural frequency are known, they can be related to the damping coefficient by realizing that a second order system can either be expressed in the form $m\ddot{x} + c\dot{x} + kx$ or the form $\ddot{x} + 2\zeta\omega_n\dot{x} + \omega_n^2 x$. A relation can therefore be made between the damping coefficient c and the natural frequency ω_n and damping ratio ζ where

$$c_{eff} = 2m\zeta\omega_n$$

Where the mass m is m_m the combined mass of the payload, carriage and 1/3 of the mass of the tip. Additionally a relation for k and ω_n can be derived

$$k_{eff} = m\omega_n^2$$

Where m is again m_m, the combined mass at the tip of the mast.

Results

After having developed a theoretical model for the forklift, the next step was to simulate the model in Matlab. The initial conditions inputted into the Matlab program are summarized in Table A1 of the Appendix. The effective stiffness and effective damping coefficient in Table 1 were then computed.

Table 1: Calculated Stiffness and Damping Coefficients

k_{eff} from geometry and material data	$1.90*10^5$ Nm
k_{eff} from experimental data	$1.87*10^4$ Nm
c_{eff} from experimental data	245 Ns/m

As can be seen above, there are significant differences in the effective stiffness using the two different methods described in the earlier section. Analysis of the results in Matlab produced the following plots.
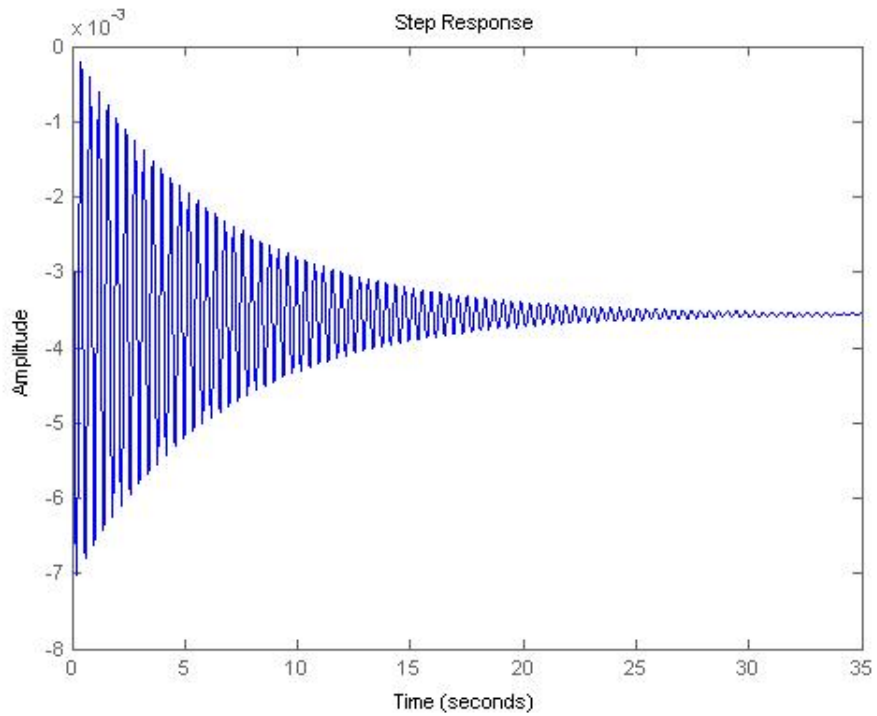
Figure 4: System derived using the effective stiffness from the geometric and material properties of mast under step response conditions.
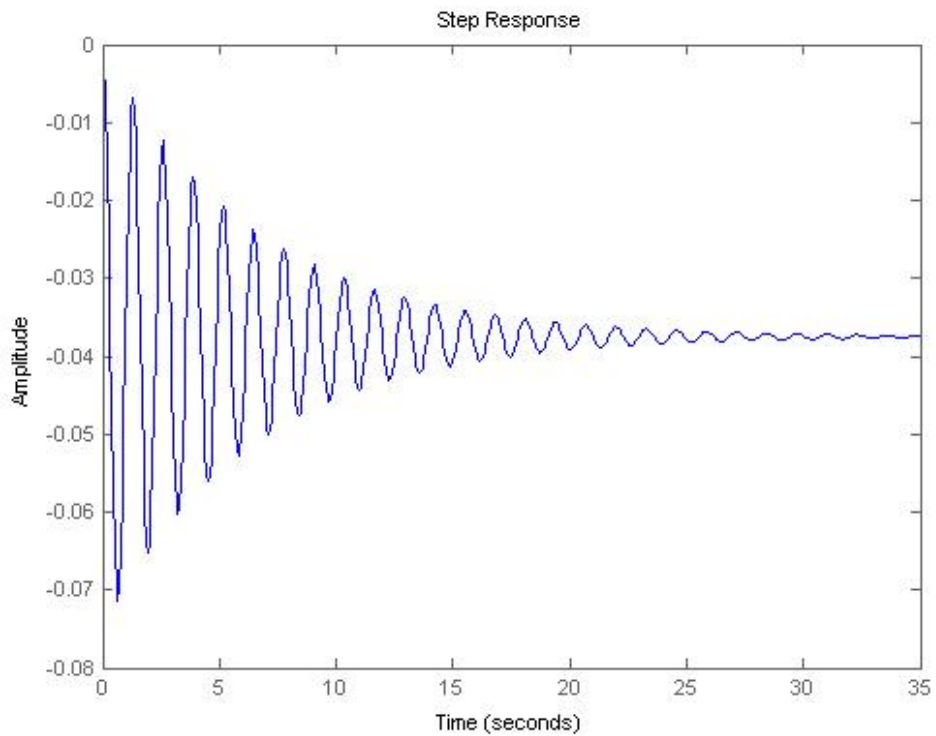

Figure 5: System derived using the effective stiffness from experimental data under step response conditions.

The effective stiffness derived from the geometry and material data is much higher than the expected natural frequency for the system and therefore it was no longer used to model the reach truck. The state space matrix derived in equations 4 and 5 was put into the Matlab code with one minor difference. The user defined input used for most analysis was a constant force required to accelerate the entire reach truck at a rate of $0.5\ m/s^2$ which is a fairly typical value for the acceleration. The B matrix was scaled to reflect a forcing input of this magnitude and make it possible to use Matlab function such as the step function in the analysis. The B matrix used in the Matlab function was therefore,

$$B = \begin{bmatrix} 0 \\ 0.5(m_t + m_m)/m_t \\ 0 \\ 0 \end{bmatrix}$$

Where $0.5(m_t + m_m)$ was the forcing function f inputted into the system. Root locus plots were also generated for the system in order to begin working on control strategies. As can be seen on the root locus plot the system has a pair of complex conjugate poles in the left half plane and two repeated poles at the origin.
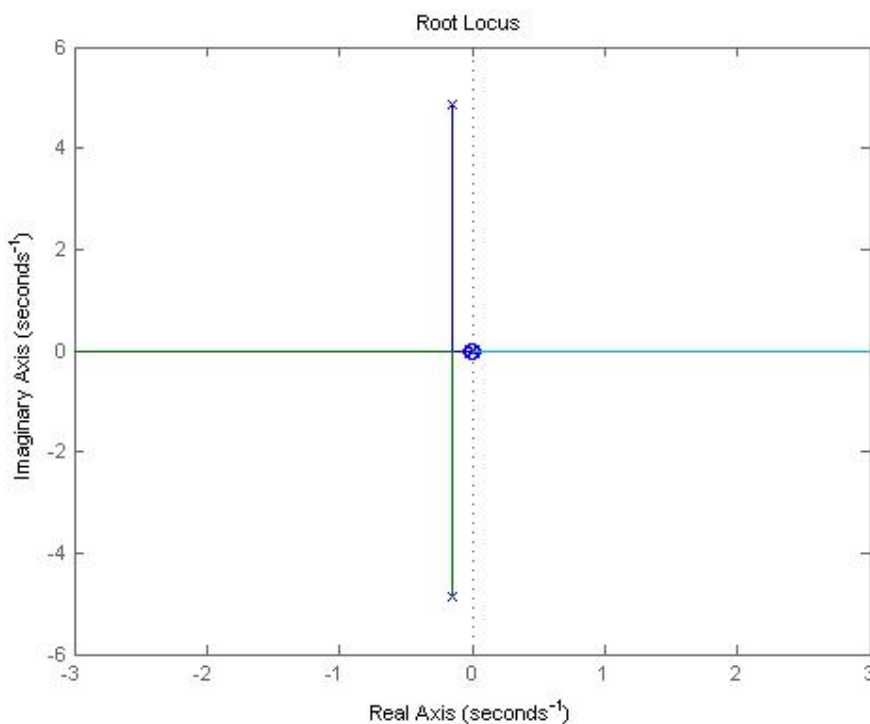
**Figure 6: Root locus plot of uncontrolled system**

The focus of this project was the vibration of the mast and the carriage when the forklift was translating; however significant vibration is likely to occur while the forklift is turning as well. The following section examines the effects of the tractor turning on the motion of the mast and carriage when the carriage is raised to its maximum height. While it is unlikely that the forklift operator would choose to turn the vehicle while the carriage is fully elevated, the following qualitative analysis predicts unstable motion of the mass and carriage if this were to occur. This type of instability needs to be addressed with further system controls to ensure the operator's safety and the customer's trust in Raymond's product.
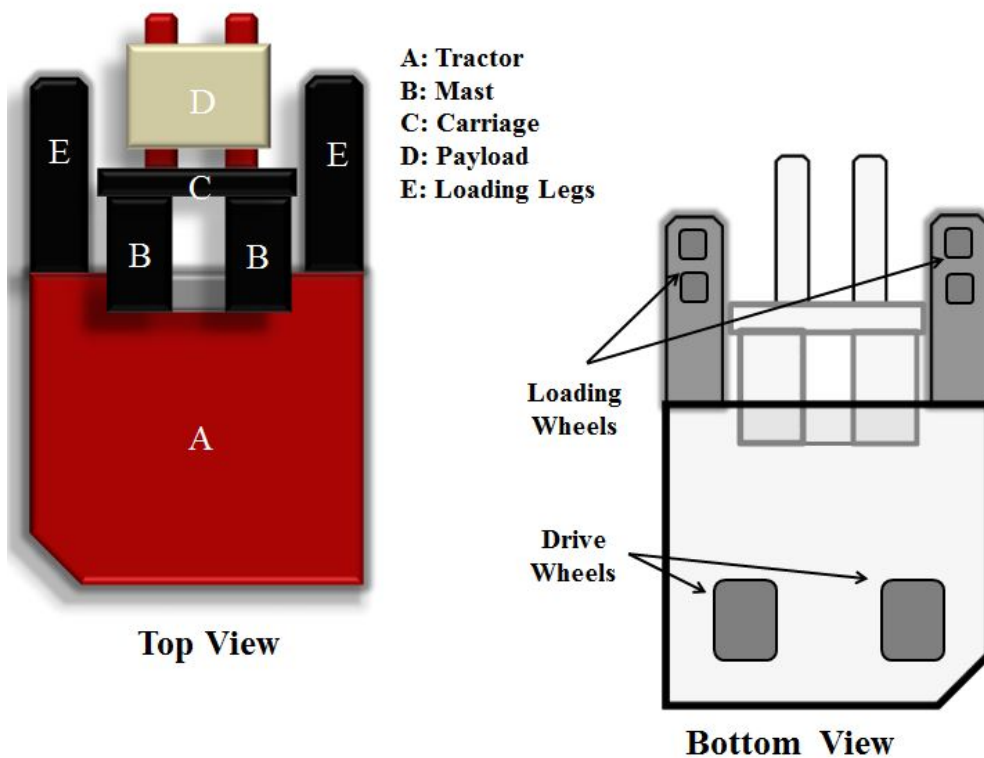
Figure 8: Schematic of the Top and Bottom of the Forklift with Relevant Sections Defined

The forklift has three degrees of freedom when turning: 1) rotation of the tractor, 2) rotation of the two mast beams and 3) rotation of the carriage. As shown in Figure 8 the forklift has six wheels, two on each loading leg and two drive wheels in the rear of the vehicle. The loading wheels then serve as pivot points for the turning motion. The rotational motion of each part is dependent on the motion of the others, creating a very complex problem.
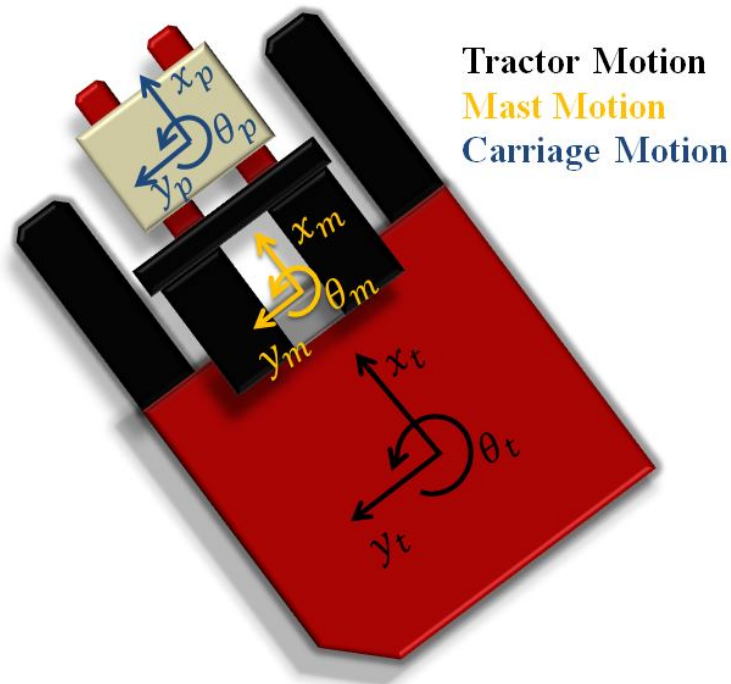
Figure 9: Definitions of Motion for Each Degree of Freedom of the Forklift

To fully define this problem, relative coordinate systems were given to each moving part as shown in Figure 9. For the purposes of this discussion the pivot point of the tractor is defined near its center of gravity rather than near the loading wheels as it would be in a real system. In order to move the forklift, the motor applies a torque to one of the drive wheels, which propels the forklift forward. Turning the steering wheel of the forklift forces the tractor to rotate, causing both rotational and translation motion in the mast and carriage. As mentioned earlier, the translational motion of the forklift causes significant oscillations of the mast and carriage in the xz plane. Rotation of the tractor is likely to cause oscillations in the yz plane. The mast telescopes have particularly small moments of inertia in the yz plane, which increases the stress and decreases the stiffness of the mast in that plane. If unconstrained, oscillations in the yz plane could be more severe than those in the xz plane. Oscillation of the carriage depends on the outreach distance of the reach ram compared to the mast. The reach ram mechanism allows the carriage to extend even further forward. At maximum extension, the reach ram changes the location for the center of gravity of the system, which makes it more vulnerable during excitations. However again, it is unlikely that the operator would choose to turn while the reach ram is fully extended.

Turning may have the largest effect on the motion of the payload itself. If the payload is not constrained while on the carriage it has the potential to slide relative to the carriage platform, which changes the center of gravity of the system and the motion of the mast. Most of the analysis that has been performed for translational motion discounts the motion of the payload itself and simply lumps the payload and carriage together as one system. In the case of turning motion, the effect of the payload on

14

the mast and the tractor cannot be discounted due to the large mass the payload can possibly undertake. Reach Truck specifications list the maximum "deep reach" capacity of the carriage to be 3,200 lbs. Given that the weight of the mast is approximately 765 lbs, the weight distribution of the entire forklift changes when the payload changes position.

Numerical Approaches

Several approaches were taken in an attempt to describe this problem mathematically; however we found that the number of unknown was far too great for a calculation at this time. More analysis needs to be performed to fully explain the system. One approach treated the connections between the tractor and the mast as well as the connection between the mast and the carriage as a torsional spring. Motion was then defined by the following torsional harmonic oscillation equation,

$$I\ddot{\theta} + C\dot{\theta} + \kappa\theta = \tau$$

where I is the mass moment of inertia of the rotating body, C is the torsional damping constant, κ is the torsional spring constant, τ is the applied torque, and θ is the rotation. Calculations were performed to find the translational damping and spring constants; however the given data was not conducive to solving for the torsional constants. Furthermore, defining the torque applied to the tractor requires a more complex analysis involving experimental data from the motor and exact dimensions of the tractor itself. Therefore, the attempt to describe this type of motion with torsional harmonic oscillation was unsuccessful.

Using an energy approach, we found the same issues with unknown parameters as before. The following Lagrange equation,

$$\frac{d}{dt}\left(\frac{\partial T}{\partial q_i}\right) - \frac{\partial T}{\partial q_i} + \frac{\partial U}{\partial q_i} = Q_i$$

where T is the kinetic energy of the ith moving part, U is the potential energy, q_i is the displacement, and Q_i represents the non-conservative forces of moments acting on the system, was used to determine the governing equations of motion for each part(Inman). Kinetic and potential energies were defined by,

$$T = \frac{1}{2}I_i\theta_i^2 + \frac{1}{2}k_ix_i^2$$

$$U = -\int \tau d\theta$$

By inserting the energies for each moving part into the Lagrange equation we found the following system of equations,

$$
\begin{bmatrix} I_t & 0 & 0 \\ 0 & I_m & 0 \\ 0 & 0 & I_p \end{bmatrix} \begin{Bmatrix} \dot{\theta}_t \\ \dot{\theta}_m \\ \dot{\theta}_p \end{Bmatrix} - \begin{bmatrix} I_t & 0 & 0 \\ 0 & I_m & 0 \\ 0 & 0 & I_p \end{bmatrix} \begin{Bmatrix} \theta_t \\ \theta_m \\ \theta_p \end{Bmatrix} - \begin{bmatrix} \tau_t & 0 & 0 \\ 0 & \tau_m & 0 \\ 0 & 0 & \tau_p \end{bmatrix} \begin{Bmatrix} d\theta_t \\ d\theta_m \\ d\theta_p \end{Bmatrix} = \begin{Bmatrix} Q_t \\ Q_m \\ Q_p \end{Bmatrix}
$$

The mass moments of inertia were previously calculated using estimated dimensions, but with the amount of information known we found that it was not possible to solve for the torque of the tractor and non-conservative moments. Internal torques, τ_m and τ_p do not affect the overall motion of the body and can be disregarded.

Further analysis needs to be performed on the torque applied to the tractor to begin rotational and translational motion. The most significant motion is likely to occur when the forklift is accelerating or decelerating; therefore being able to apply a specific number to the applied torque will significantly improve our understanding of the system Without experimental data and further numerical analysis it is difficult to conclude whether additional controls should be added to stabilize the mast and carriage while turning; however, unstable motion is highly likely if the operator were to choose to turn the vehicle with the carriage fully elevated.

Results and Discussion

After simulating the model for the reach truck in Matlab, it was discovered that the effective stiffness derived by using the geometric and material properties of the beams composing the mast did not match the expected system results. The natural frequency of the system produced suing this effective stiffness was approximately 3 times as large as it should have been according to Figures 6 and 7. This stems from the fact that the analytical calculations does not account for additional compliances in the system, such as those introduced by the loading legs. This may also be because the method used to find this effective stiffness does not take into account the position of the carriage or the mass of the payload. As can be seen in Table 2 of the Appendix, which summarizes values for the natural frequency found by Fernando Gonzalez in his report on the Orderpicker Longitudinal Mast Dynamics, variations in the position of the carriage and mass of the payload can have a significant effect.

One concern that we have is that the root locus of the open loop system contains two poles at the origin. This implies that the open loop system is unstable. And indeed, when the open loop model is

stimulated with an impulse response, the mass and tractor drift off to infinity, since there are no frictional forces in the model. Thus, open and closed loop stability cannot be easily inferred from root locus plots.

The first control strategy studied was an electronically implemented dashpot between the tractor and mast. The control action for such a system acts on the tractor and can be described as

$$F_g = -k_v(\dot{x}_m - \dot{x}_t)$$

The equations of motion for the closed loop system are then

$$\begin{bmatrix} m_t & 0 \\ 0 & m_m \end{bmatrix} \ddot{\vec{x}} + \begin{bmatrix} c_{eff} & -c_{eff} \\ -c_{eff} + k_v & c_{eff} - k_v \end{bmatrix} \dot{\vec{x}} + \begin{bmatrix} k_{eff} & -k_{eff} \\ -k_{eff} & k_{eff} \end{bmatrix} \vec{x} = \begin{bmatrix} f(t) \\ 0 \end{bmatrix}$$

Implementing this control strategy yields the following step response plot. As can be seen in Figure 10 below, the active damping appears to effectively reduce both the settling time and magnitude of the oscillations. However the system may be unstable as evidenced by the asymmetric damping matrix. This asymmetry stems from the non-collocated nature of the feedback and actuator mechanisms.
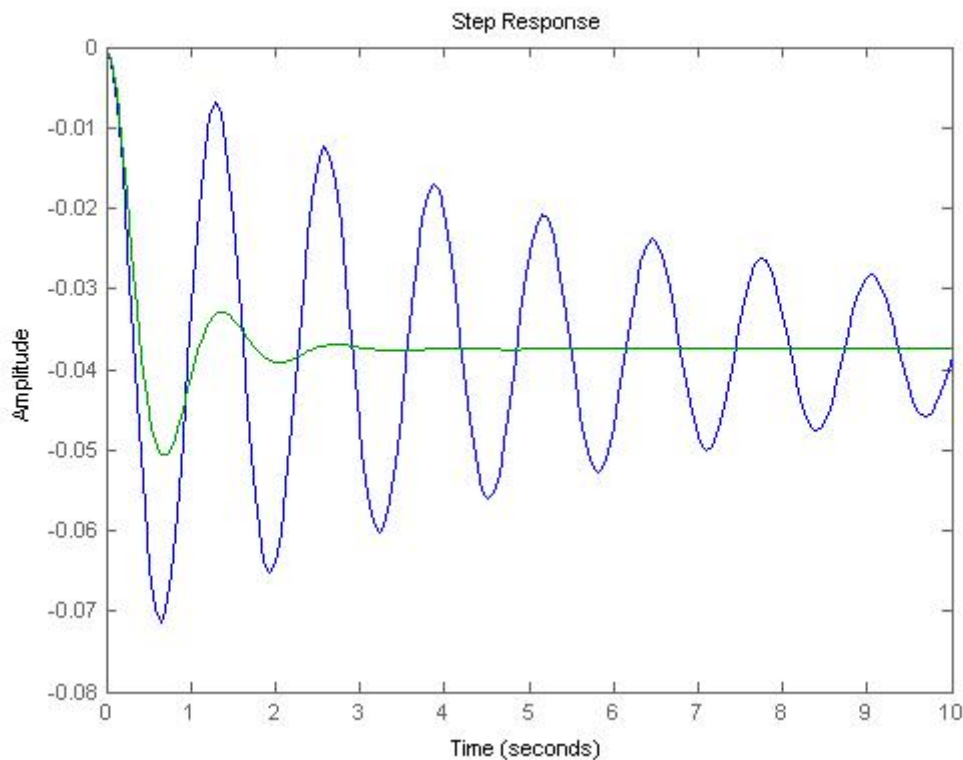
Figure 10: Comparison of uncontrolled system (blue) and controlled system using passive control damping (green) under step response conditions

Another control strategy currently being studied is the proof mass actuator control system. Proof mass actuators have had proven success in suppressing the vibrations of flexible structures (Garcia, et al.).

In the figure below m_p is the mass of the proof mass, k_p is the effective stiffness of the spring between the proof mass actuator and the effective mass at the tip of the mast and the proof mass, and c_p is the effective damping between the effective mass at the tip of the mast and proof-mass. F_g is the force generator that outputs force to create the control action.
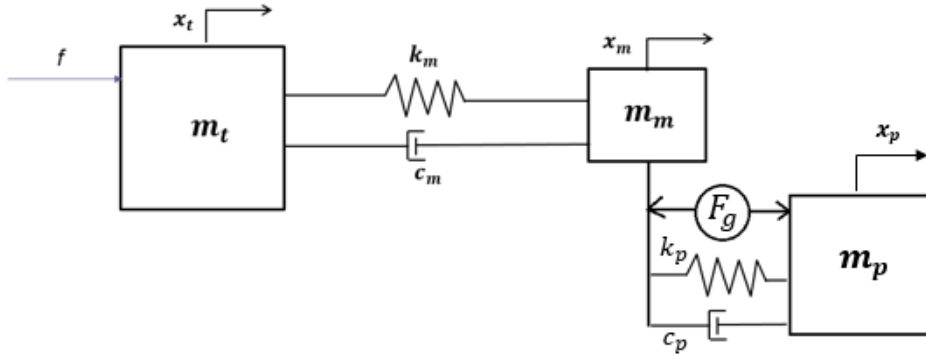
Figure 11: Proof mass actuator control system

The dynamics of the closed loop system is captured below

$$
\begin{Bmatrix} \dot{x}_t \\ \ddot{x}_t \\ \dot{x}_m \\ \ddot{x}_m \\ \dot{x}_p \\ \ddot{x}_p \end{Bmatrix} =
\begin{bmatrix}
0 & 1 & 0 & 0 & 0 & 0 \\
-\dfrac{k_m}{m_t} & -\dfrac{c_m}{m_t} & \dfrac{k_m}{m_t} & \dfrac{c_m}{m_t} & 0 & 0 \\
0 & 0 & 0 & 1 & 0 & 0 \\
\dfrac{k_m}{m_m} & \dfrac{c_m}{m_m} & -\dfrac{k_m+k_p}{m_m} & \dfrac{c_m+c_p}{m_m} & \dfrac{k_p}{m_m} & \dfrac{c_p}{m_m} \\
0 & 0 & 0 & 0 & 0 & 1 \\
0 & 0 & \dfrac{k_p}{m_p} & \dfrac{c_p}{m_p} & -\dfrac{k_p}{m_p} & -\dfrac{c_p}{m_p}
\end{bmatrix}
\begin{Bmatrix} x_t \\ \dot{x}_t \\ x_m \\ \dot{x}_m \\ x_p \\ \dot{x}_p \end{Bmatrix} +
\begin{Bmatrix} 0 \\ \dfrac{F}{m_t} \\ 0 \\ \dfrac{F_g}{m_m} \\ 0 \\ -\dfrac{F_g}{m_m} \end{Bmatrix}
$$

The next step would be to derive a state-space model for the system depending on what control strategy for F_g is used. System parameters such as k_p and c_p would need to be tuned to the systems' fundamental frequency to suck energy out of the system. We plan on investigating both passive and active control policies for the proof mass actuator in the future.

The next steps for this project are to improve the system model and develop a robust control strategy for this system model. More accurate system parameters (e.g. mass, mast height, etc.) can be obtained, and our computations can be re-done to get more accurate values. Our system model can also be made more accurate through experimental validation. Now that we have a mathematical model for the plant, we plan to explore more control strategies in the future. In particular, we hope to look more into proof mass actuator and observer-based full-state feedback. We also plan on investigating the longitudinal

reach mechanism as a control actuator and determining the physical actuator limitations needed to effectively attenuate mast vibrations.

References

- Garcia EE, Webb CS, Duke MJ. Passive and Active Control of a Complex Flexible Structure Using Reaction Mass Actuators. *J. Vib. Acoust.*. 1995;117(1):116-122.
- Goncalves, Fernando D. Orderpicker Longitudinal Mast Dynamics. Raymond Advanced Research. November 16 2011.
- Ibrahim, Ahmed M. An analytical model for the longitudinal behavior of high-lift fork trucks. Raymond Advanced Research. November 16 2011.
- Inman, Daniel J. Engineering Vibration. Published by: Prentice-Hall, Inc, 1994, in Englewood Cliffs, NY.

Appendix

System Parameters

Table A1: Summary of inputs used for Matlab code

Variable	Input
M_t	4000 lbs
M_p	1500 lbs
M_c	1088 lbs
M_{ma}	765 lbs
I_1	93 in^4
I_2	70.67 in^4
I_3	55.8 in^4
l_1	153 in
E	200 Gpa
ζ	0.0239
f_n	0.5812 Hz

Table A2: Summary of natural frequency and damping ratios found by Fernando Gonzalez in his report on the Orderpicker Longitudinal Mast Dynamics

Test Condition		Response	
Fork Height (in)	Load on Forks (lb)	ω_n (Hz)	ζ
360	0	0.616	0.0329
360	750	0.626	0.0283
360	1500	0.5812	0.0239
300	0	1.0055	0.0299
300	750	0.8582	0.0287
300	1500	0.7925	0.0378
240	0	1.4448	0.0363
240	1500	1.0814	0.0577
240	3000	0.8836	0.0573
180	0	1.8701	0.1497
180	1500	1.4652	0.0629
180	3000	1.2750	0.0500

Matlab Code

```matlab
%Nathan Woo, Alais Hewes, Megan Gould
%Raymond Corporation Project

close all
clear all
clc

%% DEFINE PHYSICAL CONSTANTS
%Define given physical parameters
Mt = 4000*.45359;           %tractor mass in Kvg
Mp = 1500*.45359;           %payload mass
Mc = 115+1088*.45359;       %carriage mass
Mm = 765 * .45359;          %mast mass

I1 = 93*.0254^4;            %Moment of inertia for bottom telescope in m^4
I2 = 70.67*.0254^4;         %Moment of inertia for middle telescope
I3 = 55.8*.0254^4;          %Moment of inertia for top telescope

l1 = 153*.0254;             %Length of bottom telescope in m
l2 = 106.5*.0254;           %Length of middle telescope
l3 = l2;                    %Length of top telescope

E = 200e9;                  %Young's Modulus of steel in Pa

zeta = 0.0239;              %damping coefficient from Fernano
wn = 0.5812;                %natural frequency in Hz from Fernando

%Calculate theoretical parameters
Mtip = 1/3*Mm + Mc + Mp;    %effective mass at mast tip
Kv1 = 3*E*I1/l1^3;          %effective stiffness of bottom telescope
```

```matlab
Kv2 = 3*E*I2/l2^3;          %effective stiffness of middle telescope
Kv3 = 3*E*I3/l3^3;          %effective stiffness of top telescope
Kv_ana = (Kv1*Kv2*Kv3)/(Kv1*Kv2 + Kv1*Kv3 + Kv2*Kv3); % effective stiffness of entire
mast
%The analytical effective mast stiffness does not account for the mass of
%the payload or the mass of the carriage. These additional masses would
%decrease the effective stiffness. We ended up using the experimental
%stifness value for the purposes of simulation.

%Calculate experimental parameters
c = 2*zeta*(wn*2*pi)*Mtip;  %damping coefficient
Kv = Mtip*(wn*2*pi)^2;       %experimental effective stiffness

%Build open loop state-space matricesh
A=[0 1 0 0; -Kv/Mt -c/Mt Kv/Mt c/Mt; 0 0 0 1; Kv/Mtip c/Mtip -Kv/Mtip -c/Mtip];
B=[0; 0.5*(Mt+Mtip)/Mt; 0; 0];
C=[-1 0 1 0];
D=0;
sys=ss(A,B,C,D);


%% CONTROLLER: DASHPOT AT TRACTOR
%Build closed loop state-space matrices (dashpot at tractor)
Kv=5000;      %Gain constant for passive damping controller

A_c=[0 1 0 0; -Kv/Mt -(c+Kv)/Mt Kv/Mt (c+Kv)/Mt; 0 0 0 1; Kv/Mtip c/Mtip -Kv/Mtip -
c/Mtip];
B_c=[0; 0.5*(Mt+Mtip)/Mt; 0; 0];
C_c=[-1 0 1 0];
D_c=0;
sys_c=ss(A_c,B_c,C_c,D_c);

%Define simulation time frame
tspan=0:0.01:10;

%Define acceleration profile of tractor
u=zeros(1,length(tspan));
for i=1:200
    u(i)=1;
end
for i=550:750
    u(i)=-1;
end

%Simulate open loop and closed loop step responses for
%pos(mast)-pos(tractor)
figure(1)
%lsim(sys,u,tspan)
hold on
step(sys,10)
step(sys_c,10)


%Simulate open loop and closed loop step responses for pos(tractor) and
%pos(mast)
C_c_t = [1 0 0 0];
C_c_m = [0 0 1 0];
sys_c_t = ss(A_c,B_c,C_c_t,D_c);
sys_c_m = ss(A_c,B_c,C_c_m,D_c);
figure(2)
impulse(sys_c_m,10)
    %both outputs blow up to infinity => dashpot controller on tractor
    %fails
```

```matlab
%Plot root locus of closed loop system
[num,den] = ss2tf(A,B,C,D);
[num_c,den_c] = ss2tf(A_c,B_c,C_c,D_c);
oltf=tf(num,den);
cltf=tf(num_c,den_c);
figure(3)
rlocus(cltf)


%Confirm pole/zero location on R-L via eigenvalues
%The CL dynamics can be described with the following equations of motion:
%Mxdotdot+Cxdot+Kvx = F
% M = [Mtip 0; 0 Mt];
% C = [c -c; (-c+Kv) (c-Kv)];
% Kv = [Kv -Kv; -Kv Kv];
% F = [0; 0.5*(Mt+Mtip)/Mt];    %Arbitrarily assume forKvlifts has a step input to
achieve 0.5m/s^2 acceleration

Mmatr = [Mt 0; 0 Mtip];
Cmatr = [(c-Kv) (-c+Kv); -c c];
Kvmatr = [Kv -Kv; -Kv Kv];
Fmatr = [0.5*(Mt+Mtip)/Mt; 0];

Amatr = [zeros(2,2), eye(2,2); -Mmatr\Kvmatr, -Mmatr\Cmatr];
[V D] = eig(Amatr)
roots(den_c)
```